ISSN: 2640-5571

Research Article

Advances in Nanoscience and Nanotechnology

Arc Plasma Deposited Copper and Gold Nanoparticles on FTO Substrate for Electrochemical Reduction of CO_2

F S Khan[1]*, M Sugiyama[1], K Fuji[2], and Y Nakano[3]

[1]*Department of Advance Interdisciplinary Studies, School of Engineering, University of Tokyo, Tokyo, Japan*

[2]*RIKEN Center for Advanced Photonics, Wako, Japan*

[3]*Department of Electrical Engineering, School of Engineering, University of Tokyo,Tokyo, Japan*

***Corresponding author**

FS Khan, Department of Advance Interdisciplinary Studies, School of Engineering, University of Tokyo, Tokyo, Japan, E-mail: fahd@hotaka.t.u-tokyo.ac.jp

Submitted: 30 Dec 2018; **Accepted**: 24 Jan 2019; **Published**: 15 Feb 2019

Abstract

A composite of copper and gold nanoparticles was deposited using arc plasma deposition on the conductive FTO substrate for the electrochemical reduction of CO_2. The use of arc plasma deposition system allows the nanoparticles to be implanted onto the substrate as opposed to the commonly used methods of vacuum deposition or electro deposition. This unique structure reduced the CO_2 to produce formic acid with up to 60% faradaic efficiency. Copper and gold nanoparticles have never previously been reported to produce formic acid with such high efficiency, suggesting that the co-deposition technique of implanted nanoparticles can provide an interesting future avenue in the field of electrochemical reduction of CO_2. The surface analysis of the electrodes is presented here along with potential dependent faradaic efficiency of the electro catalysis.

Keywords: CO_2 Reduction, Electro Catalysis, Arc Plasma Deposition, Fluorine Doped Tin Oxide, glass Substrate, Copper, Gold, Nanoparticles

Introduction

In recent past, the major policy drive led by the United Nations and governments have helped to establish institutional regimes enforcing CO_2 reduction mechanisms in public as well as private sector. Improving the performance efficiency towards lesser greenhouse gases emissions are not enough to meet the targets set by the 2015 Paris Agreement. Therefore there remains an enormous need to find new materials that could utilize the emitted CO_2 and transform it into useful products such as CH_4, CO, HCOOH etc so as to close the loop for a net-neutral carbon cycle.

The electrochemical reduction of CO_2 has been a major research direction for this utilization of CO_2. Traditionally, the focus of this electrochemical research has remained on metal electrodes as cathodes, and has been studied extensively [1-6]. The relatively simple composition and well-characterized surface offer the convenience to study CO_2 reduction over potentials and product formation mechanisms, both from theoretical and experimental perspectives.

Although many metal electrodes can be used as the cathode to catalyze CO_2 reduction reactions (CO_2RR), the over potential however is very high. Copper has remained the best performing electrode for generating carbon-intensive products however the quest for finding new electrode materials remain the new challenge and therefore, research using co-catalyst decorated electrodes and metal oxides have recently begun to gain attraction in an attempt to increase CO_2 reduction on lower potentials [7]. With the prosperity of nanotechnology and advances obtained since the late 1990s, nanostructures have emerged as a new type of material with unique advantages, such as large surface areas and high tunability in morphology as well as compositions. Various gold- and silver-based nanostructures have been synthesized and have been demonstrated as effective CO_2 electro reduction catalysts [8]. Surface engineering, morphology control, and composition manipulation to form alloy or core-shell nanostructures as well as the utilization of such structures to fabricate composites can greatly tune the catalytic properties of nanostructures, area and catalytic active sites [9-12]. As an example, the flat surfaces of the bulk gold and silver electrodes show limited activity in CO_2 reduction, but surface modification to form nanostructures on the surface of the electrodes through reducing oxidized gold and silver electrodes is an effective strategy [8].

In this study, we present the results for depositing copper (Cu) and gold (Au) nanoparticles on the conductive glass material: fluorine doped tin oxide (FTO). The Arc Plasma Deposition (APD) technique was employed to deposit the nanoparticles and is characterized by highly dispersed and uniform nanoparticles of metallic states, which exhibit high catalytic activities. These high catalytic activities, is suggested to originate from the various possible combinations of bimetal nanoparticles, which subsequently results in much more possibilities in shape and structure due to the assorted distribution

of each metal within a particle and their various organization and is the reason why bimetallic nanoparticle catalysis has been extensively used in many industrial applications [13].

On the other hand, the utilization of arc-plasma process allows simultaneous deposition of implanted Cu and Au nanoparticles. The unique catalytic properties associated with implantation of bimetals, are based on the idea that the structure and reactivity and selectivity of certain metal nanoparticles can be promoted by the other metal elements. Fluorine doped tin oxide (FTO) was chosen as the substrate material because of its conductivity as well as its disordered glass structure which can potentially allow unique reaction centers [14]. The deposition of copper and gold nanoparticles, in principle can yield a composite reaction mechanism in which the CO_2 reductions can take place on multiple sites. The reduction of CO_2 using Au electrode can primarily only generate CO and since CO is known to be an intermediate specie for carbon intensive products, it can act as a feedstock for Cu NPs [15-16]. We theorize that CO generated during CO_2RR at Au can be utilized by the neighbouring Cu NPs, and can help to reduce the number of steps for generating carbon intensive products at Cu hence raising faradaic efficiency in CO_2RR.

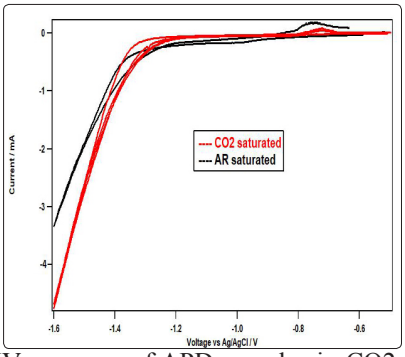

Figure 1: IV response of APD samples in CO2 and Ar saturated electrolyte

Experimental

Fluorine-doped tin oxide (FTO) is prepared through mixed quantities of SnO_2 and SnF_2. These FTO substrates were commercially procured from Sigma Aldrich vendor after which the samples were sent to Advance Riko Inc for deposition of nanoparticles (NP). Cu and Au nanoparticles were deposited on FTO by arc discharge of metallic Cu and metallic Au cathodes, respectively. All the depositions were carried out under vacuum (at 10^{-3} Pa) at room temperature. The number of arc discharge pulses (N) was 150 shots, the Capacitance of the condenser (C) was 1080 mF, and the voltage for arc discharge (V) was 134 V for Cu and 142 V for Au. In this study, it was observed after the XPS analysis that the difference in arc discharge resulted in deposition of relatively smaller Au NPs and bigger Cu NPs.

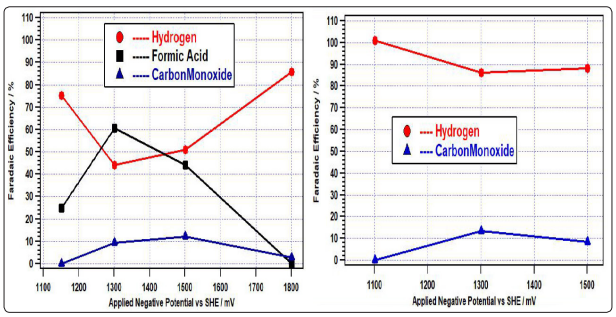

Figure 2: Faradaic efficiency against negative cathodic potential for pristine APD electrode (left) and control samples (Pristine FTO) (right)

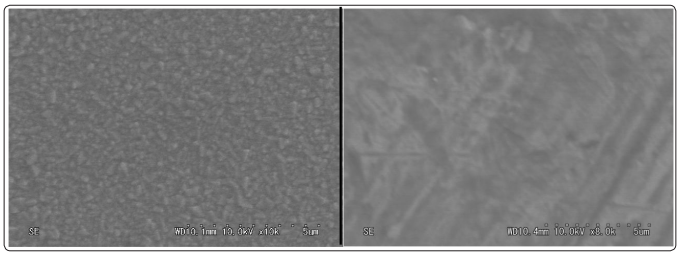

Figure 3: SEM images for pristine APD electrode (left) and stabilized APD electrode (right)

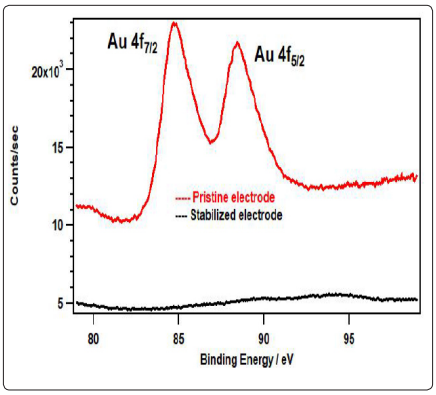

Figure 4: XPS analysis comparison for Au element in pristine and stabilized electrode

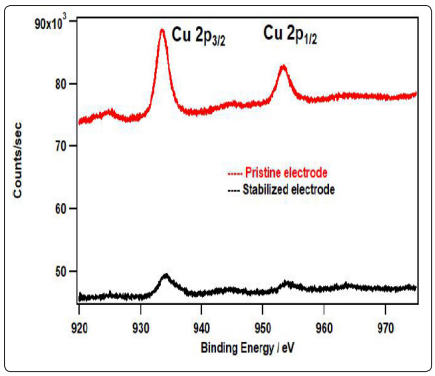

Figure 5: XPS analysis comparison for Cu element in pristine and stabilized electrode

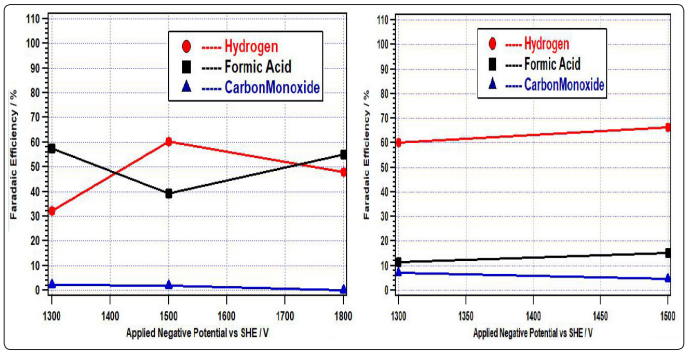

Figure 6: Faradaic efficiency against negative cathodic potential for stabilized APD electrode (left) and control electrode (stabilized FTO)(right)

Table 1: Table 1: Comparative XPS analysis for pristine and stabilized electrodes

	Carbon	Oxygen	Copper	Gold	Tin	Flourine	Silicon
Atomic Conc. for Pristine electrode / %	74.60	19.9	2.20	1.40	1.90	Below detection limit	Below detection limit
Atomic Conc. for stabilized electrode / %	61.1	28.4	2.0	Below Detection Limit	2.7	4.2	1.6

Capacitance of the condenser (C) was 1080 mF, and the voltage for arc discharge (V) was 134 V for Cu and 142 V for Au. In this study, it was observed after the XPS analysis that the difference in arc discharge resulted in deposition of relatively smaller Au NPs and bigger Cu NPs.

Home-made H-type leak-tight electrochemical cells were used for CO_2 reduction, with 100 cm3 volume and 70 ml of electrolyte. The end-products were collected for further analysis. The working and reference electrodes were put in the same compartment and separated from the counter electrode by a nafion film (DuPont: N117). Since CO_2 reduction is a redox reaction, during the reduction of CO_2, H_2O/OH- is oxidized into O_2 at the anode side and so the separation between the working and counter electrodes, helps to ensure that the recombination of the products produced on these two electrodes can be effectively prohibited. Ag/AgCl reference electrode was employed while platinum was used as the counter electrode. 0.5 M $KHCO_3$ with a pH of 8.60 was used in the cathode and anode electrolyte, which dropped to 7.20 pH in the cathode half-cell after the CO_2 purging. The pH changes were not observed during the experiment. The gas product was then sampled manually through syringe using HP 6890 Gas Chromatographer (GC).

The liquid phase products were determined by Ion Chromatography (IC) and collected with a Thermo Scientific Dionex ICS-5000 system. The X-ray emission photoelectron spectroscopy was conducted by Mg X-ray source in ULVAC-PHI 1600C to analyze the atomic concentration. Electrochemical experiments were performed using Solartron 1280C potentiostat while a stir bar was used within the electrochemical cell. Electrodes were prepared by affixing a copper wire to the substrate. The electrolyte was purged with CO_2 or Ar gas for 25 min prior to experimental or control trials, respectively.

Results and Discussion

In order to gauge the activity of the electrodes for CO_2RR, a comparative IV response was measured by using the same electrode in CO_2-saturated and Ar-saturated electrolyte, which is shown in figure 1. Enhanced current density was observed in CO_2-saturated electrolyte, which is a reflection of CO_2RR activity. The result of the CO_2RR experiments is produced in figure 2, in which hydrogen remained the dominant product along with formic acid and CO. The formic acid FE is around 21% at the onset of CO_2RR at 1150 mV vs SHE and peaks at around 60% at 1300 mV after which it slides down again to almost zero at 1800 mV vs SHE. The minor product from CO_2RR was CO production which remained below 10% however in experiments employing only the control FTO substrate as the electrode, CO remained the only product from CO_2RR while hydrogen production continued as a parasitic product. The difference between CO and HCOOH is suggested to originate from the difference of intermediate specie, that of COOH and *OCHO, respectively [17]. Chemically the intermediate species contain the same elements however local pH alterations and over potentials have been speculated to determine the outcome of the product [18]. Initially it was observed that a reddish-brown layer used to form after electrochemical experiments, indicative of surface deterioration and which increased at more negative cathodic potentials. However, after about 6 experiments, it was observed that no further substrate deterioration took place and substrate surface stability was achieved. The Scanning Electron Microscope (SEM) images in figure 3 shows the difference in surface between pristine and stabilized electrodes. The FTO glass film on pristine electrode had initially undergone deterioration after repeated experiments. The degeneration of surface partially disintegrates the thin film on the glass structure and the reddish-brown color suggests that it is SnO_2, which is subsequently cleaned off after the experiment. It was important to gauge the impact of this surface disintegration on the deposited metal NPs as well as the surface of the FTO substrate. XPS analysis was conducted on pristine and stabilized electrode surfaces to analyze the comparative differences. Figure 4 shows the comparative peak intensities for Au where the clearly identifiable Au presence in pristine electrode has been reduced to no detectable Au peak in stabilized electrode. This represented that its atomic concentration was less than the detection limit. Cu was more clearly observed (as seen in figure 5) which reflected that the size of implanted Cu NPs was larger than Au and so implantation was more anchored into the surface.

Table 1 shows the comparative analysis of the relative atomic concentrations of the surface elements. The atomic concentration of implanted Cu remained stable however the Au concentration decreased to below the detection limit. The erosion of SnO_2 meant that the presence of Sn would decrease and this can be seen in the relative increase of fluorine to tin in the stabilized electrode. Since the FTO substrate is a combination of polycrystalline SnO_2 and SnF_2, in which SnO_2 is usually the dominant entity, we speculate that the absence of detectable fluorine in the pristine electrode reflects that SnF_2 was not present within the nanometer range depth resolution of XPS and the top few nanometers of FTO is primarily composed of SnO_2 [19]. Carbon contamination on the surface from the APD fabrication process also decreased after the deterioration of the surface. Since the reaction centers for CO_2RR are suggested to be on the metal NPs and the surface continued to be conductive, the relative changes of Sn, O, F should not present a major drawback for CO_2 reduction. Post-stabilization, silicon was also observed after XPS analysis with an atomic concentration of about 1.6 %, which had originated from slight exposure of the underlying SiO_2 substrate beneath FTO, after degradation. This also explains the relative increase of oxygen, seen in the stabilized phase. The non-conductive silicon oxide substrate does not play any role in CO_2RR and the very small concentration of Si on the surface shows that the exposed substrate area was very small and cannot cause any meaningful decrease in the conductive electrode area to the electrolyte. The impact of this electro deterioration on the faradaic yields for the stabilized electrode can be seen in figure 6 for both the stabilized APD electrode as well as control FTO electrode. The

product selectivity and faradaic difference of the stabilized electrode to the control electrode, remained constant. In the stabilized phase, there was no visible physical difference in between the APD and control samples, since the atomic concentration and size of the implanted NPs was small. Formic acid was observed in control FTO substrate as well however the FE remained lower than that of APD electrode. The origin of formic acid in the control sample is suggested to be from the SnO_2 in the disintegrated surface, which as reported in previous studies, does produce formic acid in CO_2RR experiments [20]. FTO substrates are considered chemically inert and mechanically hard in ambient conditions however the flow of electrons in the liquid electrolyte partially disintegrates the surface structure upon which the exposure of sub-surface SnO_2 also takes place, increasing the surface area exposure to the electrolyte and hence facilitating formic acid production.

Conclusion

Arc plasma Deposition was employed to implant Cu and Au NPs on to the surface of FTO. The electrochemical experiments showed formic acid generation with FE as high as 60% while CO was observed as a secondary product. AES and XPS spectroscopy confirmed the atomic concentration and presence of the NPs deposition. Pristine FTO was used as control electrodes and produced only CO as a result of CO_2RR. Surface degradation of FTO substrate was a parasitic result from the application of negative cathodic potential in bicarbonate electrolyte however the surface reached an equilibrium state after which no visible disintegration was observed. The control FTO electrode had started to produce formic acid in the electrode-stabilization phase however the FE towards formic acid in stabilized APD electrodes continued in relatively much higher yields.

References

1. Frese Jr KW, Sullivan BP, Krist K, Guard HE (1993) Electrochemical Reduction of CO_2 at Solid Electrodes. In Electrochemical and Electro catalytic Reactions of Carbon Dioxide. Eds; Elsevier 145-216.
2. Sánchez-Sánchez CM, Montiel V, Tryk DA, Aldaz A, Fujishima A (2001) Electrochemical Approaches to Alleviation of the Problem of Carbon Dioxide Accumulation. Pure Appl Chem 73: 1917-1927.
3. Lvov SN, Beck JR, LaBarbera MS, Muradov NZ, Veziroglu TN (2012) Electrochemical Reduction of CO_2 to Fuels. In Carbon-Neutral Fuels and Energy Carriers, CRC Press 363-400.
4. Lu X, Leung DYC, Wang H, Leung MKH, Xuan J (2014) Electrochemical Reduction of Carbon Dioxide to Formic Acid. Chem Electro Chem 1: 836-849.
5. Le MTH (2011) Electrochemical Reduction of CO_2 to Methanol. Master's Thesis, Louisiana State University,
6. Solar Thermochemical Process Technology http://www.academia.edu/4353252/Solar_Thermochemical_Process_Technology .
7. V. S. K. Yadav, M. K. Purkait, Electrochemical reduction of CO_2 to HCOOH using zinc and cobalt oxide as electrocatalysts, RSC Adv. 2015, 5, 40414
8. Shuo Zhao, Renxi Jin, Rongchao Jin (2018) Opportunities and Challenges in CO_2 Reduction by Gold- and Silver-Based Electrocatalysts. Bulk Metals to Nanoparticles and Atomically Precise Nanoclusters, ACS Energy Lett 3: 452-462.
9. Koh JH, Jeon HS, Jee MS, Nursanto EB, Lee H et al., (2015) Oxygen Plasma Induced Hierarchically Structured Gold Electrocatalyst for Selective Reduction of Carbon Dioxide to Carbon Monoxide. J Phys Chem C 119: 883-889.
10. Chen Y, Li CW, Kanan MW (2012) Aqueous CO_2 Reduction at Very Low Over potential on Oxide-Derived Au Nanoparticles. J Am Chem Soc 134: 19969-19972.
11. Mistry H, Choi YW, Bagger A, Scholten F, Bonifacio CS et al., (2017) Enhanced Carbon Dioxide Electroreduction to Carbon Monoxide over Defect-Rich Plasma-Activated Silver Catalysts. Angew Chem 129: 11552-11556.
12. Ma M, Trzesn-iewski BJ, Xie J, Smith WA (2016) Selective and Efficient Reduction of Carbon Dioxide to Carbon Monoxide on Oxide-Derived Nanostructured Silver Electrocatalysts. Angew Chem Int Ed 55: 9748-9752.
13. Magda Blosi, Simona Ortelli, Anna Luisa Costa, Michele Dondi, Alice Lolli et al., (2016) Bimetallic Nanoparticles as Efficient Catalysts: Facile and Green Microwave Synthesis Materials (Basel) 9: 550.
14. Hiroya Homura, Osamu Tomita, Masanobu Higashi, Ryu Abe (2017) Fabrication of CuInS2 photocathodes on carbon microfiber felt by arc plasma deposition for efficient water splitting under visible light, Sustainable Energy Fuels 1: 699-709.
15. Wenlei Zhu, Ronald Michalsky, O_nder Metin, Haifeng Lv, Shaojun Guo et al., (2013) Monodisperse Au Nanoparticles for Selective Electro catalytic Reduction of CO_2 to CO. J Am Chem Soc 135: 16833-16836.
16. Schouten KJP, Kwon Y, van der Ham CJM, Qin Z, Koper MTM (2011) a new mechanism for the selectivity to C1 and C2 species in the electrochemical reduction of carbon dioxide on copper electrodes. Chem Sci 2 1902.
17. Raciti D, Mao M, Park JH, Chao Wang (2018) J Electrochem Soc volume 165, issue 10, F799-F804.
18. Jeremy T Feaster, Chuan Shi, Etosha R Cave, Toru Hatsukade, David NAbram et al., (2017) ACS Catal 7: 4822-4827.
19. Ziad Y Banyamin, Peter J Kelly, Glen West, Jeffery Boardman (2014) Electrical and Optical Properties of Fluorine Doped Tin Oxide Thin Films Prepared by Magnetron Sputtering, Coatings 4: 732-746.
20. Shaolin Mu, Jun Wu, Qiaofang Shi, Fengmin Zhang (2018) Electro catalytic Reduction of Carbon Dioxide on Nano sized Fluorine Doped Tin Oxide in the Solution of Extremely Low Supporting Electrolyte Concentration: Low Reduction Potentials. ACS Appl Energy Mater 4: 1680-1687.